

Periodic Mesoporous Organosilicas: A Type of Hybrid Support for Water-Mediated Reactions

Ying Wan,^{*,[a]} Dieqing Zhang,^[a] Yunpu Zhai,^[b] Cuimiao Feng,^[a] Jia Chen,^[a] and Hexing Li^{*,[a]}

Abstract: Hybrid mesoporous periodic organosilicas (Ph-PMOs) with phenylene moieties embedded inside the silica matrix were used as a heterogeneous catalyst for the Ullmann coupling reaction in water. XRD, N₂ sorption, TEM, and solid-state NMR spectroscopy reveal that mesoporous Ph-PMO supports and Pd/Ph-PMO catalysts have highly ordered 2D hexagonal mesostructures and covalently bonded organic-inorganic (all Si atoms bonded with carbon) hybrid frameworks. In the Ullmann coupling reaction of iodobenzene in water, the yield of biphenyl

was 94 %, 34 %, 74 % and for palladium-supported Ph-PMO, pure silica (MCM-41), and phenyl-group-modified Ph-MCM-41 catalysts, respectively. The selectivity toward biphenyl reached 91 % for the coupling of bromobenzene on the Pd/Ph-PMO catalyst. This value is much higher than that for Pd/Ph-MCM-41 (19 %) and Pd/MCM-41 (0 %), although the conversion of bro-

mobenzene for these two catalysts is similar to that for Pd/Ph-PMO. The large difference in selectivity can be attributed to surface hydrophobicity, which was evaluated by the adsorption isotherms of water and toluene. Ph-PMO has the most hydrophobic surface, and in turn selectively adsorbs the reactant haloaryls from aqueous solution. Water transfer inside the mesochannels is thus restricted, and the coupling reaction of bromobenzene is improved.

Keywords: catalyst • supports • hydrophobic effect • mesoporous materials • organosilicas • water

Introduction


Periodic mesoporous organosilicas (PMOs), which were first reported in 1999, are synthesized by replacing the precursor tetraethoxysilane (TEOS) with a bridged organosilsesquioxane through the surfactant self-assembly approach analogous to that used in the preparation of ordered mesoporous silicates.^[1–6] The structures of the pore walls are composed of tetrahedrally coordinated silicon centers bridged with

oxygen atoms and organic groups.^[1–3] Unlike functionalized mesoporous silicates, in which the organic ligands are anchored in or onto the pore walls, PMOs demonstrate a unique organic-group distribution inside the inorganic pore walls. This type of hybrid material therefore does not contain the slitlike and bottle-neck pores that guarantee fast and efficient mass transport of species.^[7] Both chain and ring organic compounds have been integrated into inorganic matrices, including methylene, ethane, ethylene, benzene, ethylbenzene, 4-phenyl ether, 4-phenyl sulfide, and so on.^[7–10] These organic ligands within the matrix display characteristics similar to those of organic molecules. Simultaneously, the silica component of PMOs endows on them both structural rigidity and a degree of hydrophilic character.

Although much is known of the synthesis of PMOs, the number of applications that exploit their hybrid nature is limited.^[7] Much effort has been spent on developing packing materials for chromatography and adsorbents. For example, Olkhoviyk and Jaroniec synthesized isocyanurate-containing PMOs that can adsorb up to 1.8 g of Hg²⁺ per gram of adsorbent.^[11] The high affinity to contaminant cations is strongly related to the chelating or complexing agents rather than the hybrid nature of the PMOs. The potential of PMO-

[a] Prof. Dr. Y. Wan, D. Zhang, C. Feng, J. Chen, Prof. Dr. H. Li
Department of Chemistry
Shanghai Normal University
100 Guilin Road, Shanghai 200234 (China)
Fax: (+86) 21-64322272
E-mail: ywan@shnu.edu.cn
hexing-li@shnu.edu.cn

[b] Y. Zhai
Department of Chemistry
Shanghai Key Laboratory of Molecular Catalysis and Innovative Materials
Fudan University
Shanghai 200433 (China)

 Supporting information for this article is available on the WWW under <http://www.chemasianj.org> or from the author.

based materials as candidates in catalysis has also been investigated.^[12–18] Inagaki and co-workers fabricated Pt nanowires embedded in PMO frameworks and used them as catalysts for CO oxidation in the presence of excess oxygen.^[12] The turnover frequency was only slightly higher than that of nanowires inside mesoporous silicate frameworks. By using a laboratory-made bridged organosilsesquioxane as precursor, Corma et al. synthesized a PMO material that contained a carbopalladacycle complex.^[14] They found that this type of catalyst exhibits higher activity in the Suzuki coupling reaction than amorphous silica grafted with the carbopalladacycle. When functionalized with sulfonic acid or arene sulfonic groups, PMOs can serve as acidic catalysts in several types of reactions.^[15–18] For example, PMO-SO₃H can catalyze the alkylation of phenol with 2-propanol. The catalytic activity is much larger than that of microporous aluminosilicate molecular sieves ZSM-5 but similar to that of sulfonic acid modified MCM-41 (MCM-41-SO₃H) with a pure inorganic-silica matrix.^[15] The mesopore structures or the chelating agents themselves were studied instead of the hybrid organic/inorganic nature. The difference in the adsorption and catalytic properties between PMOs and mesoporous silica anchored with organic moieties is worthy of investigation.

Organic reactions in water have been extensively investigated for the fine-chemical and pharmaceutical industries, because they offer the possibility of providing environmentally benign reaction conditions by lowering the burden of organic-solvent disposal.^[19–21] Therefore, the development of new catalysts that allow reactions to be conducted in the presence of water is important for both economical and environmental concerns. In this paper, we report the use of PMOs as a novel type of catalyst support for organic reactions in water and compare Ph-PMO with pure silica MCM-41 and MCM-41 modified with phenyl groups (Ph-MCM-41). The coupling reaction of haloaryls to biphenyls is chosen as an example, which is of significance in the production of various agrochemicals and pharmaceuticals. Such reactions are usually carried out in organic solvents such as

N,N-dimethylformamide and toluene. Phenylene-containing Ph-PMO displays a unique hybrid nature that is inherited from the homogeneously distributed organic phenylene groups inside the pore walls and the inorganic silicate moieties, as well as a uniform pore-size distribution without obvious pore blockage. The Ph-PMO support has the ability to adsorb selectively a large amount of organic molecules containing the benzene ring in water, and, in turn, the Pd/Ph-PMO catalyst exhibits high catalytic activity in the water-mediated Ullmann coupling reaction. As such, we envision that this unique hybrid inorganic/organic framework will find wide application in environmentally benign catalysis.

Results and Discussion

Phenylene-containing Ph-PMOs were synthesized by surfactant self-assembly and were subsequently supported with palladium ions by impregnation. After reduction under a hydrogen-containing atmosphere, palladium-supported catalysts were obtained. Meanwhile, Pd/MCM-41 and Pd/Ph-MCM-41 were prepared by similar procedures. The small-angle XRD patterns for the solvent-extracted Ph-PMO support and the Pd/Ph-PMO catalyst are shown in Figure 1. Three well-resolved diffraction peaks are indexed as 10, 11, and 20 reflections associated with the *P6mm* hexagonal mesostructure for both materials. The XRD data indicate that the highly ordered 2D hexagonal mesostructure is obtained for Ph-PMO materials and retained after supporting palladium. The unit-cell dimensions of the hexagonal lattice for Ph-PMO and Pd/Ph-PMO were calculated to be 6.58 and 6.03 nm, respectively. The shrinkage of the domain may be related to the deposition of palladium and high-temperature reduction. The XRD patterns show that pure silica and MCM-41 with pendant phenyl groups and their corresponding Pd-containing catalysts also have highly ordered 2D hexagonal mesostructures (see Supporting Information, Figure S1). The wide-angle XRD pattern (Figure 1, inset) of the Pd/Ph-PMO catalyst shows three weak diffraction peaks

Abstract in Chinese:

本文将含苯基周期性介孔氧化硅 (Ph-PMO) 作为多相催化剂载体用于水介质中 Ullmann 偶联反应。XRD, TEM, NMR 和 N₂ 等温吸附等技术表明 Ph-PMO 载体和 Pd 负载 Ph-PMO 催化剂具有有序度高的介孔结构及有机-无机杂化性质。在以水为介质的碘苯偶联反应中, 采用 Pd/Ph-PMO 为催化剂时, 联苯的最佳得率为 94%。而在 Pd 负载的苯基杂化介孔氧化硅 (Pd/Ph-MCM-41) 和纯硅 (Pd/MCM-41) 催化剂上, 联苯的得率仅分别为 74% 和 34%。当反应物为溴苯时, 虽然在上述三种催化剂上溴苯的转化率相似, 但 Pd/Ph-PMO 上联苯的选择性为 91%, 大大高于 Pd/Ph-MCM-41 (19%) 和 Pd/MCM-41 (0%)。这可能是由于表面疏水性质的差异所致。Ph-PMO 具有最强的表面疏水性, 可以选择性吸附水中的有机反应物; 与此同时, 疏水表面限制了水在孔道中的扩散, 因此提高了催化反应活性。

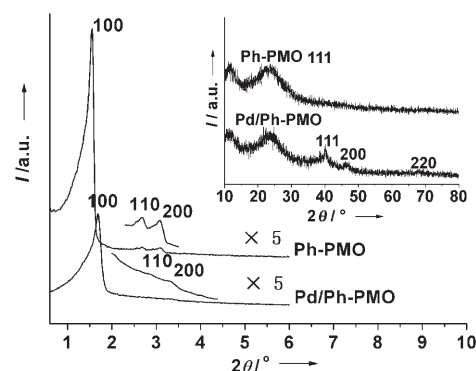


Figure 1. Small-angle XRD patterns for the Ph-PMO support with phenylene moieties embedded inside the silica matrix and the palladium-supported catalyst Pd/Ph-PMO. Inset: corresponding wide-angle XRD patterns.

at $2\theta = 40.1$, 46.5 , and 68.0° , which correspond to the (111), (200), and (220) reflections of the face-centered cubic (fcc) Pd lattice, respectively. One broad reflection at $2\theta = 24^\circ$ in both solvent-extracted Ph-PMO and the Pd/Ph-PMO catalyst can be assigned to amorphous silica, similar to that in the pure silica MCM-41. These results indicate that the frameworks of Ph-PMO are composed of amorphous walls that are different from materials with molecular periodicity in the pore walls, which are prepared by using the same bridged organosilsesquioxane as precursor and cationic surfactant as template. This phenomenon is in accordance with that reported by Inagaki and co-workers.^[8,22] The XRD reflections for Pd metal are broad, which indicates the presence of relatively small palladium nanoparticles in the catalyst. By using H_2 - O_2 titration, the size of the Pd nanoparticles was estimated to be about 1.9 nm on the basis of the spherical model.

Both the Ph-PMO support and the Pd/Ph-PMO catalyst exhibited large domains of ordered arrays in their TEM images (see Supporting Information, Figure S2), thus further revealing the high degree of hexagonal mesoscopic organization. In the case of the Pd/Ph-PMO catalyst, energy-dispersive X-ray spectroscopy (EDS) revealed the presence of palladium. The representative low-magnification TEM image of this catalyst reveals almost no obvious aggregation of nanoparticles, thus suggesting that palladium particles disperse well in the silica matrix (Figure S2). A loading of 6 wt % Pd per gram of Ph-PMO was established by inductively coupled plasma atomic emission spectroscopy (ICP-AES).

The ^{13}C cross-polarized magic-angle spinning (CP MAS) NMR spectra of the Ph-PMO support before and after solvent extraction are shown in Figure 2a. The synthesized Ph-PMO material displayed a strong resonance at 133.6 ppm along with sidebands (labeled with asterisks), which can be ascribed to carbon atoms in the benzene ring sandwiched by silicon atoms.^[8,22] Signals at 30 and 70 ppm are attributed to the carbon atoms of the surfactants. After solvent extraction, the maintenance of the first strong resonance at 133.6 ppm proves the integrity of the organic fragment in the silica matrix. The disappearance of the latter two signals indicates almost complete removal of the surfactants by acidified ethanol extraction. The two resonances at 18 and 58 ppm are due to carbon atoms from ethanol that was possibly trapped and underwent surface esterification during solvent extraction. The ^{29}Si MAS NMR spectra (Figure 2b) of the synthesized and solvent-extracted Ph-PMOs show three characteristic T^m signals assigned to Si species covalently bonded to carbon atoms T^1 ($\text{C}-\text{Si}(\text{OSi})(\text{OH})_2$; $\delta = -61.5$ ppm), T^2 ($\text{C}-\text{Si}(\text{OSi})_2(\text{OH})$; $\delta = -71.5$ ppm), and T^3 ($\text{C}-\text{Si}(\text{OSi})_3$; $\delta = -81$ ppm). No distinct signals assigned to the Q^n groups ($\text{Si}(\text{OSi})_n(\text{OH})_{4-n}$) of the silicates were observed between -90 and -120 ppm, which confirms the absence of carbon-silicon cleavage of the $\text{Si}-\text{C}_6\text{H}_4-\text{Si}$ moiety inside the frameworks during synthesis and solvent extraction. These results indicate that the frameworks consist of covalently bonded organic-inorganic networks of the

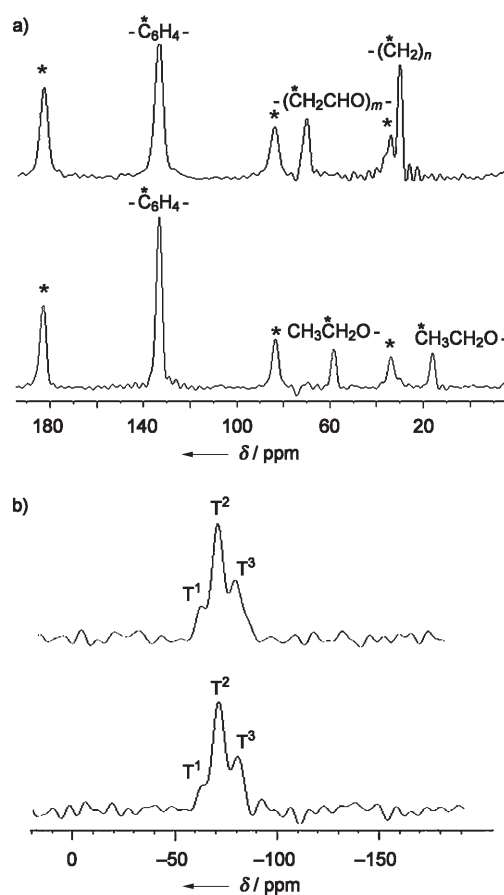


Figure 2. a) ^{13}C and b) ^{29}Si NMR spectra of the synthesized (top) and solvent-extracted (bottom) Ph-PMO supports.

$\text{O}_{1.5}\text{Si}-\text{C}_6\text{H}_4-\text{SiO}_{1.5}$ unit. The ^{13}C CP MAS NMR spectrum (see Supporting Information, Figure S3) of the phenyl-group-anchored Ph-MCM-41 material shows resonances corresponding to the phenyl functional groups (134.9 and 127.5 ppm). The ^{29}Si MAS NMR spectrum (Figure S4) of this material reveals the Q^n and T^m silica species, thus indicating the presence of phenyl groups on the silica pore walls. By assessing their relative intensities, it is possible to determine the approximate formula of the product by $\text{SiO}_{1.58}(\text{OH})_{0.48}(\text{C}_6\text{H}_5)_{0.2}$ loading of the pendant phenyl groups in Ph-MCM-41 within about 20 %.

The intensities of absorptions below 3000 cm^{-1} in the FTIR spectra of Ph-PMO (see Supporting Information, Figure S5) decreased dramatically after solvent extraction. This phenomenon suggests the elimination of the aliphatic moieties of the surfactant, in accordance with the NMR spectroscopic results. Simultaneously, the maintenance of the absorptions at 1634 and 1448 cm^{-1} attributed to organic phenylene moieties and at 1000 – 1100 cm^{-1} assigned to inorganic $\text{Si}-\text{O}-\text{Si}$ frameworks suggest the formation of an inorganic-organic hybrid matrix and its preservation during solvent extraction. After incorporation of palladium, the organic groups and inorganic frameworks remain intact, as evidenced by the presence of the characteristic vibrations. The

disappearance of adsorptions below 3000 cm^{-1} reveals the complete decomposition of the residue surfactants during the reduction of the metal catalyst at 280°C in the forming gas.

Thermogravimetric curves (see Supporting Information, Figure S6) confirm that the Ph-PMO material has high thermal stability and that the phenylene groups bridged to the frameworks can be preserved up to 500°C ; this is similar to the reported benzene-containing PMOs.^[8,22] The small weight loss between 200 and 400°C is probably due to the removal of trace surfactant or further condensation of the silanol groups.

N_2 sorption isotherms (Figure 3) of the hybrid Ph-PMO support and Pd/Ph-PMO catalyst show representative type IV curves indicative of uniform mesopores. The calculated Brunauer–Emmett–Teller (BET) surface areas are 968 and $851\text{ m}^2\text{ g}^{-1}$ for Ph-PMO and Pd/Ph-PMO, respectively. Uniform pore-size distributions with an average diameter of 3.2 and 2.8 nm were estimated by the Barrett–Joyner–Halenda (BJH) method with the adsorption branches. The total pore volumes are 0.85 and $0.66\text{ cm}^3\text{ g}^{-1}$ for the Ph-PMO support and Pd/Ph-PMO catalyst, respectively. The decrease in BET surface area, pore size, and pore volume after the impregnation of Pd in the Ph-PMO material is possibly due to the anchorage of metal nanoparticles inside the pore channels. Typical type IV nitrogen sorption isotherms were also detected for MCM-41 and Ph-MCM-41 (see Sup-

porting Information, Figure S7). Their BET surface areas, pore sizes, and pore volumes (Table 1) are 1543 and $989\text{ m}^2\text{ g}^{-1}$, 2.4 and 1.9 nm, and 0.91 and $0.51\text{ cm}^3\text{ g}^{-1}$, respectively. After modification of the phenyl groups on the silica pore walls, the nanospace is occupied, as evidenced by the decrease in pore volumes and surface areas.

Table 1. Physical properties of pure and phenyl-group-anchored mesoporous silicas and Ph-PMOs with phenylene moieties embedded in the silica framework.

Adsorbate	Parameter	MCM-41	Ph-MCM-41	Ph-PMO
Nitrogen	d_{100} [nm]	4.0	3.7	5.7
	S_{BET} [$\text{m}^2\text{ g}^{-1}$]	1543	989	968
	Pore diameter [nm]	2.4	1.9	3.2
	Pore volume [$\text{cm}^3\text{ g}^{-1}$]	0.91	0.51	0.85
	Wall thickness [nm]	2.2	2.3	3.4
Water	K ($\times 10^{-5}$)	0.86	0.43	0.34
	S_{BET} [$\text{m}^2\text{ g}^{-1}$]	200	116	439
	Pore diameter [nm]	4.4	9.0	9.2
	p/p_0	0.443	0.588	0.742
	θ [°]	29	49	68
	c	7.98	7.80	2.28
Toluene	K ($\times 10^{-5}$)	1.19	2.02	2.44
	S_{BET} [$\text{m}^2\text{ g}^{-1}$]	414	432	470
	c	3.24	34.35	111.44

The Ullmann coupling reaction of iodobenzene in water was chosen as a probe reaction to evaluate the activities of supported palladium catalysts (Table 2). Only the coupling

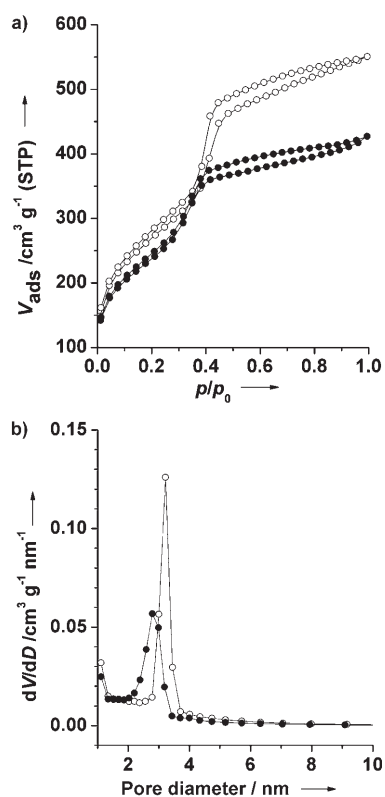


Figure 3. a) Nitrogen-sorption isotherms and b) pore-size distribution curves for the Ph-PMO support (○) and the Pd/Ph-PMO catalyst (●).

Table 2. Catalytic performance of palladium-supported MCM-41, Ph-MCM-41, and Ph-PMO.

Catalyst	PhI			PhBr		
	Conv. [%]	Sel. [%]	Yield [%]	Conv. [%]	Sel. [%]	Yield [%]
Pd/MCM-41	60	57	34	84	0	0
Pd/Ph-MCM-41	75	98	74	84	22	19
Pd/Ph-PMO	95	99	94	93	98	91

product biphenyl and the hydrodehalogenation by-product benzene were detected for all the catalysts. Pd/Ph-PMO with organic phenyl groups embedded in the inorganic silica matrix displayed the highest conversion of iodobenzene and yield of biphenyl, reaching 95 and 99%, respectively. The Pd/Ph-MCM-41 catalyst with organic moieties anchored on the pore walls showed a lower conversion of 75%, but a similar, high yield of biphenyl of 98%; the pure silica MCM-41-based catalyst exhibited the lowest catalytic activity: 60% conversion and 57% yield. The coupling reactions of bromobenzene were also tested with different catalysts, and the catalytic activities are compiled in Table 2. Pd/Ph-PMO showed a high conversion of bromobenzene (93%) and yield of biphenyl (98%). This is more valuable as bro-

mobenzene is cheaper than iodobenzene. By comparison, 84% conversion of bromobenzene and 22% yield of biphenyl was detected for Pd/Ph-MCM-41. The yield was four times less than that for Pd/Ph-PMO, although it is almost the same for the two catalysts in the coupling reaction of iodobenzene. In the case of MCM-41 as support, almost no bromobenzene was converted into biphenyl. Only benzene was detected, which suggests that hydrodehalogenation occurred in all cases.

It has been proved that palladium in the catalyst is the active site for the Ullmann coupling reaction of haloaryls. This type of coupling reaction occurs by two consecutive single-electron-transfer processes.^[21,23] An organopalladium intermediate, for example, I-Pd-Ar, is formed by oxidative addition of the catalyst to the aryl halide. Insertion then takes place to form a diarylated palladium moiety. Finally, reductive elimination gives the biaryl product and the palladium(0) species to complete the catalytic cycle. By contrast, the side reaction of dehalogenation occurs probably through nucleophilic substitution of I-Pd-Ar by HCOO⁻ anion in solvent followed by decomposition to benzene. Therefore, oxidative addition and nucleophilic substitution are the competing reactions.^[21,23] On the basis of this mechanism, the metallic palladium sites may not have a pronounced effect on the selectivity. As all the catalysts have a palladium loading of about 6 wt%, the large discrepancy in the selectivity of the Ullmann coupling reaction of haloaryls, in particular, bromobenzene, is possibly related to the nature of the supports. All the supports have highly ordered 2D hexagonal mesostructures. On the other hand, highly ordered palladium-supported phenyl-functionalized mesoporous silica catalyst Pd/Ph-SBA-15 (space group *P6mm*, characterization not shown) with a pore size of 4.4 nm shows a similar catalytic performance to Pd/Ph-MCM-41, which has a pore size of 1.9 nm. This indicates that pore size may not be the key issue affecting the catalytic properties for the Ullmann coupling reaction of iodobenzene and bromobenzene. It therefore implies that the large difference between the catalysts is mainly caused by surface properties, namely, the hybrid hydrophilic/hydrophobic character.

The hydrophilic/hydrophobic nature of Ph-PMO, Ph-MCM-41, and MCM-41 was characterized by adsorption isotherms with both water and toluene vapor. Figure 4 shows that the water adsorption isotherms are of type V, which is indicative of weak adsorbent–adsorbate interactions.^[24] At low relative pressures, the adsorption amount is low. The Henry constants for the three adsorbents calculated from the isotherm data at low pressures are listed in Table 1, which reflect the adsorption affinity. The Henry constants for water decrease in the order MCM-41 > Ph-MCM-41 > Ph-PMO. This indicates that pure silica MCM-41 has a higher affinity for water than phenyl-group-modified mesoporous silica. It is possible that the different degree of surface hydrophobicity leads to the discrepancy in the affinity sequence. The intrinsic hydrophobic property of both Ph-MCM-41 and Ph-PMO probably originates from the phenyl groups. Ph-PMO has a more-hydrophobic nature than Ph-

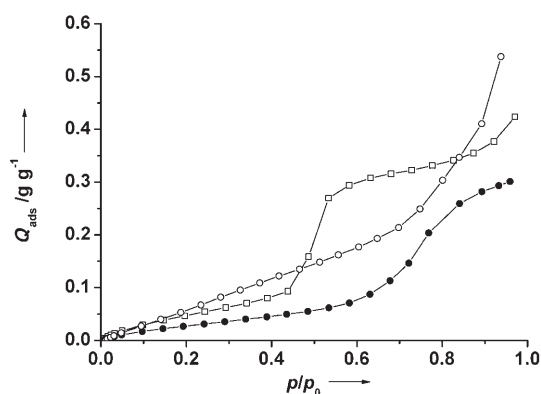


Figure 4. Water-adsorption isotherms of mesoporous pure silica MCM-41 (□), silica anchored with phenyl groups (Ph-MCM-41) (●), and silica embedded with phenylene moieties inside the pore walls (Ph-PMO) (○) at 25 °C.

MCM-41. This result may be explained by the embedding of phenylene groups inside the silica frameworks instead of their anchoring on the pore walls. The relatively regular arrangement of phenyl groups inside the pore walls results in a more-hydrophobic surface. By contrast, the hydrophobic benzene moieties are randomly distributed in Ph-MCM-41 owing to mixing, diffusion, and differences in the hydrolysis and condensation rates of the precursors.^[25] The affinity of water to the surface is thus decreased to some extent.

A steep increase in adsorption occurred at medium relative pressures of 0.45–0.75, which suggests capillary condensation. The condensation steps occurred at higher relative pressures than those in nitrogen adsorption isotherms. However, mesoporous silicas modified with organic groups have larger shifts in p/p_0 values than MCM-41. This value is extremely large for Ph-PMO, which has an indistinct capillary-condensation step at a p/p_0 value of 0.74. The shift could be attributed to the change in contact angle between the surface and water due to the difference in hydrophobicity.^[26] The calculated contact angles (Table 1) increased from 29 through 49 to 68° in the order MCM-41, Ph-MCM-41, and Ph-PMO. This order reflects the sequence of increasing hydrophobicity on the surface of these mesoporous silicas.

The change in hydrophobicity after the modification of the phenyl groups is confirmed by the toluene adsorption isotherms (Figure 5). Both MCM-41 and Ph-MCM-41 display type I toluene isotherms. In the case of Ph-PMO, the isotherm is a typical type IV curve with a distinct increase in adsorption in the p/p_0 range 0.4–0.7 owing to the filling of toluene in the mesopores. Kapoor et al.^[22] also found that the capillary-condensation step of benzene is related to the surface properties of mesoporous silicas. A shift of this equilibrium to the right suggests a more-hydrophobic surface. Therefore, Ph-PMO is more hydrophobic than the others. The pore size was calculated to be 8.4 nm, which is larger than the value estimated from nitrogen sorption isotherms. The affinity for toluene was also evaluated with the Henry constants (Table 1), which dramatically increase in the order Ph-PMO > Ph-MCM-41 > MCM-41. The phenylene groups

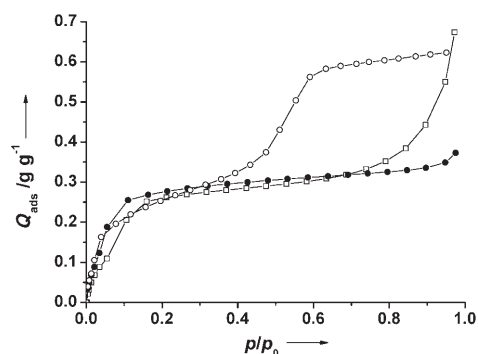


Figure 5. Adsorption isotherms of toluene vapor on MCM-41(□), Ph-MCM-41 (●), and Ph-PMO (○) at 25°C.

embedded inside the silica pore walls improve the affinity for toluene to a larger extent than those anchored on the pore walls (Ph-MCM-41). The ratios of the Henry constants (or the selectivity) for toluene to those of water at 25°C were estimated to be 1.39, 4.69, and 7.20 for MCM-41, Ph-MCM-41, and Ph-PMO, respectively. This result indicates that Ph-PMO has the greatest potential for the separation of toluene from water at moderate temperatures.

The c constant is useful for evaluating the interaction between adsorbent and adsorbate. The c constants are 111.44, 34.35, and 3.24 for Ph-PMO, Ph-MCM-41 and MCM-41, respectively, which suggests that Ph-PMO has a strong interaction with toluene molecules. Local adsorption occurs, and the effective sectional area of adsorbate reflects the size of the adsorption site instead of the real molecular size of the adsorbate. This leads to large calculated pore sizes, which are in good agreement with the above estimate.

Thus, the diffusion and adsorption of reactants and water inside the mesochannels are different. The adsorption of haloaryls is improved owing to the strong interaction between the surface and the substrate, whereas the adsorption of water is inhibited in the hydrophobic mesochannels of Pd/Ph-PMO. This character, together with the pore accessibility to palladium nanoparticles, results in the high conversion of haloaryls and the high yield of biphenyl. The Pd/Ph-PMO catalyst was also tested for reusability. It was reused at least four times in the Ullmann coupling reaction of iodobenzene without obvious loss in both conversion and yield (see Supporting Information, Figure S8). The XRD pattern for the Pd/Ph-PMO catalyst shows only minor changes after four cycles (Figure S9), thus indicating the maintenance of the highly ordered mesostructure. These results suggest that the Pd/Ph-PMO catalyst is stable in basic hot water, possibly owing to its high surface hydrophobicity.

The low activity of the Pd/MCM-41 catalyst can be explained by the restrictions of iodobenzene transfer inside the relatively hydrophilic mesopores of MCM-41. On the other hand, the coverage of water on the active sites may facilitate nucleophilic substitution and inhibit the selectivity of the catalyst. In the case of more-active bromobenzene, direct reduction to benzene is more likely to occur rather than the coupling reaction to biphenyl. For the Pd/Ph-

MCM-41 catalyst, the hydrophobic surface favors the diffusion of haloaryls and inhibits the diffusion of water inside the mesochannels to some extent. High activity was obtained when iodobenzene was used as the reactant. However, the yield of biphenyl was as low as 19% in the coupling reaction of bromobenzene, much lower than the value for the Pd/Ph-PMO catalyst.

Conclusions

The palladium-supported Ph-PMO catalyst exhibited excellent catalytic performance for the Ullmann coupling reaction of iodobenzene and bromobenzene in water. The yield of biphenyl reached 95 and 91%, respectively, whereas the yield was 0 and 19% in the coupling reaction of bromobenzene on pure silica MCM-41 and Ph-MCM-41, respectively. The ratios of the Henry constants (or the selectivity) for toluene to those for water at 25°C increased in the order MCM-41, Ph-MCM-41, and Ph-PMO, thus reflecting an increasing ability in the selective adsorption of toluene from water. It is the pore accessibility and the unique hybrid sandwiched inorganic–organic framework of Ph-PMO that contribute to the hydrophobic surface and, in turn, the high affinity for hydrophobic organic molecules. These features make it possible to extend this type of PMO hybrid catalyst to other organic reactions in water.

Experimental Section

Chemicals

Oligomeric nonionic surfactant Brij76 ($C_{18}H_{37}EO_{10}$) and high-purity toluene were purchased from Aldrich Chemical Inc. 1,4-bis(triethoxysilyl)benzene and phenyltriethoxysilane were obtained from Gelest Chemical Inc. Other chemicals were purchased from the Shanghai Chemical Company. All these chemicals were used as received without any further purification. Millipore water was used in all experiments.

Preparation of Catalysts

Ph-PMO was prepared by hydrothermal synthesis. Brij76 (2.0 g) was dissolved in water (93.5 mL) with stirring. The solution was heated to 50°C, and HCl (6.6 mL, 37 wt%) was added. After 12 h, 1,4-bis(triethoxysilyl)benzene (5.3 g) was poured in with rigorous stirring, and the mixture was kept at the same temperature for another 12 h. The resulting mixture was then transferred into a stainless-steel autoclave and heated at 90°C for 24 h. After it was cooled, the white precipitate was recovered by filtration and dried at 80°C overnight. Thereafter, the products were treated with HCl (1 M)/ethanol (350 mL g⁻¹ of solid) under stirring to extract the surfactant.

Ph-MCM-41 was synthesized according to the procedure given in the literature.^[27] TEOS (9.01 mL) and phenyltriethoxysilane (1.88 mL) was added in turn to a mixture of *n*-tetradecyltrimethylammonium bromide (2.4 g), NaOH (24 mL, 1.0 M), and distilled water (84 mL). After stirring for 48 h, the slurry solids were filtered, washed, dried in vacuum at 100°C for 10 h, and extracted with HCl (1 M)/ethanol to remove the surfactant. For the purpose of comparison, MCM-41 was also prepared by using the established procedure.^[28]

Supported palladium catalysts were prepared by isochoric impregnation of the above mesoporous silica supports with an aqueous solution of PdCl₂. Ethanol was used as the cosolvent to enhance the diffusion of palladium ions in aqueous solution into the pores of the PMOs and Ph-

MCM-41. After impregnation, the catalysts were dried at 100°C and reduced at 280°C in forming gas (10% H₂ in nitrogen) for 3 h.

Characterization

Powder XRD was carried out on a Rigaku D/Max-RB diffractometer with Cu_{Kα} radiation. The samples were loaded on a sample holder with a depth of 1 mm. N₂ adsorption isotherms were recorded at −196°C with a Nova 3000 analyzer. The catalysts were outgassed at 120°C overnight before measurement. The catalyst pore-size distribution was calculated by using the BJH formula. The specific surface area (*S*_{BET}) of the samples was determined from the linear part of the BET plot (*p/p*₀=0.05–0.25). H₂–O₂ titration experiments were conducted on a Quantachrome Chem-BET-3000 system, during which all samples were pretreated with H₂ gas flow at room temperature for 2 h. The catalysts were analyzed with ICP-AES to determine the palladium content. TEM experiments were conducted on a JEOL 2011 microscope operating at 200 kV. Samples for TEM were suspended in ethanol and supported on a holey-carbon film on a Cu grid. EDS was performed on a Philips EDAX instrument. FTIR spectra were recorded on a Nicolet Magna 550 IR spectrometer with KBr pellets of the solid samples. Weight changes of products were monitored by using a Mettler Toledo TGA-SDTA851 analyzer (Switzerland) from 25 to 900°C under nitrogen with a heating rate of 5°C min^{−1}. ¹³C solid-state CP MAS NMR and ²⁹Si solid-state MAS NMR spectra were recorded on a Bruker DRX-400 NMR spectrometer with adamantane and Q₈M₈ [(CH₃)₃SiO]₈Si₈O₁₂) as a reference, respectively.

Adsorption Tests

Adsorption-equilibrium measurements were performed by using a digital microbalance (CAHN Instrument, model D-200) with a sensitivity of 0.1 µg. Isotherm measurements were carried out by introducing a dosed amount of high-purity toluene or water vapor directly into the sample chamber and recording the weight change after stable equilibrium pressure was reached. Consecutive measurements were made by stepwise increase of the vapor pressure. Before isotherm measurements were carried out, the sample was heated to 100°C for at least 3 h in a high-vacuum system. The temperature was then gradually raised to 250°C and maintained constant for at least 6 h. Once the sample weight remained constant, the sample was cooled to the required experimental temperature. The contact angles θ were calculated by using the corrected Kelvin equation as follows: $\ln(p/p_0) = -2\gamma V_L \cos\theta / [(r - t_m)RT]$, in which *p/p*₀ is the relative vapor pressure at capillary condensation, γ and *V*_L are the surface tension and molar volume of the liquid in bulk values at the measured temperature, respectively, *t*_m is the thickness of multilayer adsorption, *R* is the gas constant, and *T* is the absolute temperature.

Catalytic Tests

Ullmann coupling of iodobenzene in water was chosen to test the activities of Pd/mesoporous silica catalysts. In a typical reaction, iodobenzene (0.91 g), water (10 g), sodium formate (1.1 g), potassium hydroxide (1.4 g), and the supported palladium catalyst (0.5 g) were placed in a closed vessel under reflux. After 10 h of stirring at 100°C, the products were analyzed by a gas chromatograph (Agilent 1790) equipped with a JWDB-5 (5% diphenyl)(95% dimethyl)polysiloxane column and an FID detector. The analysis was repeated at least three times for all tests, and the experimental errors were within ±5%. After the reaction, the Pd/Ph-PMO catalyst was separated, washed with toluene and water, and then dried under vacuum. It was then reused with fresh solvent and reactants for further runs with the same reaction conditions maintained.

Acknowledgements

This work was supported by the NSF of China (20407014 and 20521140450) and the Shanghai Science, Technology, and Education Committee (03QF14037 and T0402).

- [1] S. Inagaki, S. Guan, Y. Fukushima, T. Ohsuna, O. Terasaki, *J. Am. Chem. Soc.* **1999**, *121*, 9611.
- [2] T. Asefa, M. J. MacLachan, N. Coombs, G. A. Ozin, *Nature* **1999**, *402*, 867.
- [3] B. J. Melde, B. T. Holland, C. F. Blanford, A. Stein, *Chem. Mater.* **1999**, *11*, 3302.
- [4] J. S. Beck, J. C. Vartuli, W. J. Roth, M. E. Leonowicz, C. T. Kresge, K. D. Schmitt, C. T. W. Chu, D. H. Olson, E. W. Sheppard, S. B. McCullen, J. B. Higgins, J. L. Schlenker, *J. Am. Chem. Soc.* **1992**, *114*, 10834.
- [5] D. Y. Zhao, J. L. Feng, Q. S. Huo, N. Melosh, G. H. Fredrickson, B. F. Chmelka, G. D. Stucky, *Science* **1998**, *279*, 548.
- [6] J. Fan, C. Z. Yu, T. Gao, J. Lei, B. Z. Tian, L. M. Wang, Q. Luo, B. Tu, W. Z. Zhou, D. Y. Zhao, *Angew. Chem.* **2003**, *115*, 3254; *Angew. Chem. Int. Ed.* **2003**, *42*, 3146.
- [7] F. Hoffmann, M. Cornelius, J. Morell, M. Froba, *J. Nanosci. Nanotechnol.* **2006**, *6*, 265.
- [8] S. Inagaki, S. Guan, T. Ohsuna, O. Terasaki, *Nature* **2002**, *416*, 304.
- [9] M. P. Kapoor, S. Inagaki, *Chem. Mater.* **2002**, *14*, 3509.
- [10] W. J. Hunkes, G. A. Ozin, *Chem. Mater.* **2004**, *16*, 5465.
- [11] O. Olkhoviyk, M. Jaroniec, *J. Am. Chem. Soc.* **2005**, *127*, 60.
- [12] A. Fukuoka, H. Araki, Y. Sakamoto, S. Inagaki, Y. Fukushima, M. Ichikawa, *Inorg. Chim. Acta* **2003**, *350*, 371.
- [13] A. Corma, H. Garcia, *Adv. Synth. Catal.* **2006**, *348*, 1391.
- [14] A. Corma, D. Das, H. Garcia, A. Leyva, *J. Catal.* **2005**, *229*, 322.
- [15] X. D. Yuan, H. I. Lee, J. W. Kim, J. E. Yie, J. M. Kim, *Chem. Lett.* **2003**, *32*, 650.
- [16] Q. H. Yang, J. Liu, J. Yang, M. P. Kapoor, S. Inagaki, C. Li, *J. Catal.* **2004**, *228*, 265.
- [17] Q. H. Yang, M. P. Kapoor, S. Inagaki, N. Shirokura, J. N. Kondo, K. Domen, *J. Mol. Catal. A* **2005**, *230*, 85.
- [18] S. Hamoudi, S. Royer, S. Kaliaguine, *Microporous Mesoporous Mater.* **2004**, *71*, 17.
- [19] R. Noyori, M. Aoki, K. Sato, *Chem. Commun.* **2003**, 1977.
- [20] T. Tsukinoki, H. Tsuzuki, *Green Chem.* **2001**, *3*, 37.
- [21] Y. Wan, J. Chen, D. Q. Zhang, H. X. Li, *J. Mol. Catal. A* **2006**, *258*, 89.
- [22] M. P. Kapoor, N. Setoyama, Q. H. Yang, M. Ohashi, S. Inagaki, *Langmuir* **2005**, *21*, 443.
- [23] S. Venkatraman, C. J. Li, *Tetrahedron Lett.* **2000**, *41*, 4831.
- [24] F. Rouquerol, J. Rouquerol, K. Sing in *Adsorption by Powders and Porous Solids*, Academic Press, London, **1999**.
- [25] S. R. Hall, C. E. Fowler, B. Lebeau, S. Mann, *Chem. Commun.* **1999**, 201.
- [26] S. Inagaki, Y. Fukushima, *Microporous Mesoporous Mater.* **1998**, *21*, 667.
- [27] S. L. Burkett, S. D. Sims, S. Mann, *Chem. Commun.* **1996**, 1367.
- [28] Y. Wan, H. X. Ma, Z. Wang, W. Zhou, *Microporous Mesoporous Mater.* **2004**, *76*, 35.

Received: February 18, 2007

Revised: April 3, 2007

Published online: June 5, 2007